DOI: 10.26599/FSHW.2026.9251239

Contents lists available at SciOpen

Food Science and Human Wellness

journal homepage: https://www.sciopen.com/journal/2097-0765

China Food Publishing Co.

Comparative screening identifies *Lanmaoa asiatica* polysaccharide as the most potent edible bolete polysaccharide against colorectal cancer with NRF2-GPX4-related redox imbalance

Qing Hu[a], Caiyun Zhang[a], Rongrong Sun[a], Mengyao Xia[a], Hao Meng[a], Huizhi Wang[a], Jianming Luo[a]*, Xichun Peng[a]*

[a]*Department of Food Science and Engineering, Jinan University, Guangzhou 510632, Guangdong, China*

ABSTRACT: Colorectal cancer (CRC) is one of the most common malignancies worldwide and remains a major cause of morbidity and mortality. Polysaccharides from edible boletes (BPs) have been reported to possess antitumor activity, but their direct effects on CRC remain poorly understood. In this study, polysaccharides derived from *Suillus bovinus* (SBP), a *Boletus* sp. closely related to *B. recapitulatus* (BP), *Lanmaoa asiatica* (LMP), and a *Boletus* sp. closely related to *B. edulis* (BEP) were evaluated in an AOM/DSS-induced mouse model and CRC cell lines. All four polysaccharides exhibited antitumor activity, with LMP showing the strongest effects. *In vitro*, LMP markedly inhibited HT-29 cell proliferation by suppressing DNA synthesis and inducing G1-phase cell cycle arrest. Mechanistically, LMP treatment was associated with reduced NRF2 and GPX4 expression, accompanied by ROS accumulation, oxidative stress, and DNA damage, while elevated HO-1 protein levels may reflect a redox-related adaptive response. Our findings suggest that redox-related mechanisms are involved in the antitumor effects of *Boletus* polysaccharides, and that LMP shows potential as a functional food ingredient for colorectal cancer prevention.

Keywords: Colorectal cancer; Boletus polysaccharides; *Lanmaoa asiatica* polysaccharides; cell proliferation; cell cycle arrest; oxidative stress; redox imbalance

1. Introduction

Colorectal cancer (CRC), as the third most commonly diagnosed cancer and the second leading cause of cancer-related death worldwide, poses a significant global health burden. While traditionally considered a disease of older adults, the incidence of CRC has been increasing among younger populations in recent years[1,2]. The World Health Organization has emphasized that maintaining a healthy lifestyle is an effective primary prevention strategy for CRC[3]. Among lifestyle-related determinants, dietary patterns play a particularly important role. High consumption of processed meats and low intake of fruits and vegetables increase CRC risk[4], accumulating evidence indicates that dietary patterns rich in dietary fiber are associated with a reduced risk of CRC[5].

***Corresponding author**
luojm@jnu.edu.cn; tpxchun@jnu.edu.cn

Received 18 November 2025
Received in revised from 4 January 2026
Accepted 30 April 2026

Non-starch polysaccharides (NSPs) are a class of natural active components abundant in the Mediterranean diet. They are known for their excellent anti-inflammatory and immunomodulatory activities, and have been shown to improve ulcerative colitis through multiple pathways[6]. For example, ginger polysaccharides can significantly inhibit the proliferation of HCT116 colon cancer cells[7]. *Hericium erinaceus* polysaccharides are able to induce apoptosis in HCT116 and DLD1 colon cancer cells by triggering the caspase-9-dependent intrinsic mitochondrial signaling cascade[8]. Additionally, *Ganoderma lucidum* polysaccharides have been shown to alleviate tumor genesis in Azoxymethane/Dextran sulfate sodium-induced mice[9]. A key characteristic of NSPs is that they are generally not digested in the small intestine but instead serve as an energy source for the gut microbiota in the large intestine. The byproducts of this fermentation, such as short-chain fatty acids, modulate gut function and regulate systemic health via the gut-organ axis[10]. Despite accumulating evidence of NSPs' antitumor potential, most studies focus on their indirect effects via modulation of the gut microbiota. However, polysaccharides are often not completely degraded[11]. Direct effects of NSPs on tumor cells *in vivo* remain relatively unexplored. NSPs have been shown to interact with macrophage surface receptors in the intestinal, modulating immune responses[12]. This suggests that NSPs could also contribute directly to antitumor activity.

Edible boletes are edible fungi primarily distributed in temperate and subtropical regions of the Northern Hemisphere, including Europe, Asia, and North America. It is rich in various nutrients and bioactive substances[13]. *Boletus*-derived polysaccharides (BPs) have been shown to possess antitumor activity. Acidic polysaccharides from *Boletus edulis* can inhibit the proliferation of breast cancer cells MDA-MB-231 and Ca761[14]. BPs and their glycoproteins are able to modulate the cell cycle and specifically inhibit the growth of the LS180 colon adenocarcinoma cell line[15]. Due to their potential health-promoting effects, BPs are considered a promising source for functional foods and pharmaceuticals that warrant further investigation. However, the antitumor activity and underlying mechanisms can vary among different types of BPs. It is important to explore and compare them in order to identify BPs with superior antitumor potential. To provide a more targeted comparison, four edible boletes with different levels of prior evidence were selected. *Lanmaoa asiatica* was prioritized because our preliminary work suggested antioxidant activity. *Suillus bovinus* was also included because its polysaccharides have been reported to possess antioxidant activity, suggesting potential relevance to redox regulation[16]. An edulis-related *Boletus* sample was also included because polysaccharides from *Boletus edulis* have been reported to exhibit antitumor activity[17]. A *Boletus* sample closely related to *B. recapitulatus* was selected as commonly consumed market mushrooms for which direct evidence of anti-colorectal cancer activity remains limited.

In this study, we aimed to investigate the preventive potential of polysaccharides from four selected edible boletes against CRC and to explore the underlying mechanisms. We compared the *in vitro* and *in vivo* direct antitumor activities of different BPs and identified the most potent one, LMP. Our findings suggest that LMP may help prevent CRC development through redox-related effects, providing a scientific basis for their potential application as a functional food ingredient for CRC prevention.

2. Results

2.1 Comparative antitumor activities of different bolete polysaccharides in vitro

The effect of different BPs on the CRC cell lines HT-29 and CT26 viability was evaluated using the CCK-8 assay (Fig. 1). The results showed that all four types of mushroom polysaccharides could inhibit the proliferation of HT-29 cells in a concentration-dependent manner. Among them, LMP had the most significant inhibitory effect, with an inhibition rate of 32.91% at a concentration of 800 μg/mL. BEP was the second most effective, with an inhibition rate of 28.39% at the same concentration. The inhibition rate for BP was 10.05%. In contrast, SBP showed the weakest antitumor activity, with a relatively weak inhibitory effect only at 800 μg/mL and an inhibition rate of approximately 12.52% (Fig. 1A-D).

At the same concentration, SBP and BP had no significant inhibitory effect on the viability of CT26 mouse colon cancer cells. However, LMP and BEP showed some inhibitory effects, with inhibition rates of 18.87% and 24.22% respectively at a concentration of 800 μg/mL (Fig. 1E-H).

Furthermore, a toxicity evaluation on normal colon cells revealed that SBP, BP, and LMP were not toxic to NCM460 cells within the experimental concentration range. However, BEP showed slight cytotoxicity at a concentration of 800 μg/mL (Fig. 1I-L).

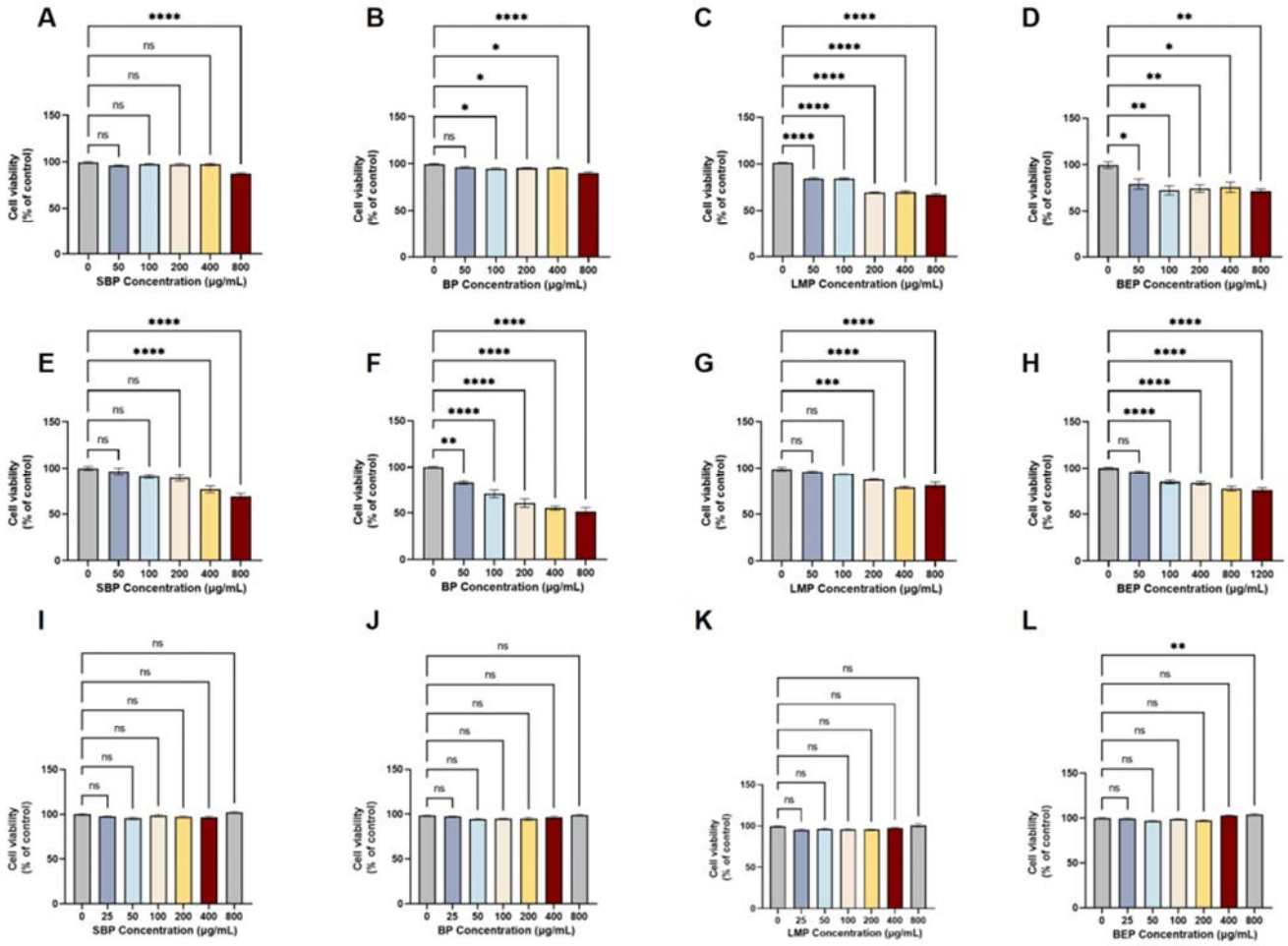

Fig. 1 The impact of different bolete polysaccharides on cell viability. (A-D) HT-29 cells viability. (E-H) CT26 cells viability. (I-L) NCM460 cells viability. Data are expressed as mean ± SD (n =3). *$P < 0.05$, **$P < 0.01$, ***$P < 0.001$ by One-way ANOVA.

2. 2 The effects of four bolete polysaccharides on colon cancer

The AOM/DSS-induced colorectal cancer model typically involves the induction of DNA mutations in colon epithelial cells by AOM, followed by DSS-induced chronic colitis to promote tumor formation. DSS-induced colitis leads to colon fibrosis and tissue shrinkage, which manifests as colon shortening. In this model, colon length is positively correlated with the severity of inflammation and/or tumor burden.

Representative images showed that the colons in the model group exhibited more obvious macroscopic lesions than those in the control group, whereas these lesions appeared alleviated to different extents after treatment with Boletus polysaccharides (Fig. 2A–B). Compared with the control group, the colon length of mice in the model group was significantly reduced. Treatment with polysaccharides alleviated this shortening to varying degrees. Among them, LMP showed the most pronounced restorative effect, while BEP, GLP, and SBP also significantly increased colon length relative to the model group. BP showed only a modest improvement (Fig. 2F). Analysis of tumor number revealed that polysaccharides significantly inhibited AOM/DSS-induced colorectal tumor formation. The order of tumor burden was Mod > SBP > BEP > BP > GLP > LMP, indicating that LMP exerted the strongest inhibitory effect on tumor development (Fig. 2E).

Histopathological examination showed that the colonic mucosa in the model group exhibited obvious erosion and ulceration, accompanied by fibrous granulation tissue proliferation, inflammatory necrosis, glandular hyperplasia, goblet cell reduction, and inflammatory cell infiltration, whereas these pathological alterations were alleviated to varying degrees in the polysaccharide-treated groups (Fig. 2C). In addition, Ki67 immunohistochemical staining suggested increased proliferative activity in the model group, which was attenuated after polysaccharide treatment, particularly in the LMP and GLP groups (Fig. 2D).

Myeloperoxidase (MPO) can generate reactive oxygen species and is commonly elevated in cancer patients, making it a potential biomarker for colon cancer. The results showed that as colon cancer progressed, oxidative stress levels increased, and the MPO activity in the blood of the model group was significantly higher than that of the control group. However, SBP, BP, LMP, BEP, and GLP polysaccharides were all able to significantly inhibit the increase in MPO activity caused by the colon cancer model (Fig. 2G).

Tumor necrosis factor-α (TNF-α) and interleukin-6 (IL-6) synergistically facilitate the proliferation of colon cancer cells, suppress cellular apoptosis, and potentiate their invasive and metastatic capacities, thereby serving as pivotal drivers in the initiation and progression of colon cancer. The results demonstrated that, with the exception of the SBP group, all other experimental groups exerted a downregulatory effect on TNF-α expression in the colonic tissues of mice; notably, the SBP, LMP, and GLP groups were capable of reducing IL-6 expression in the colonic mucosa (Fig. 2H-I).

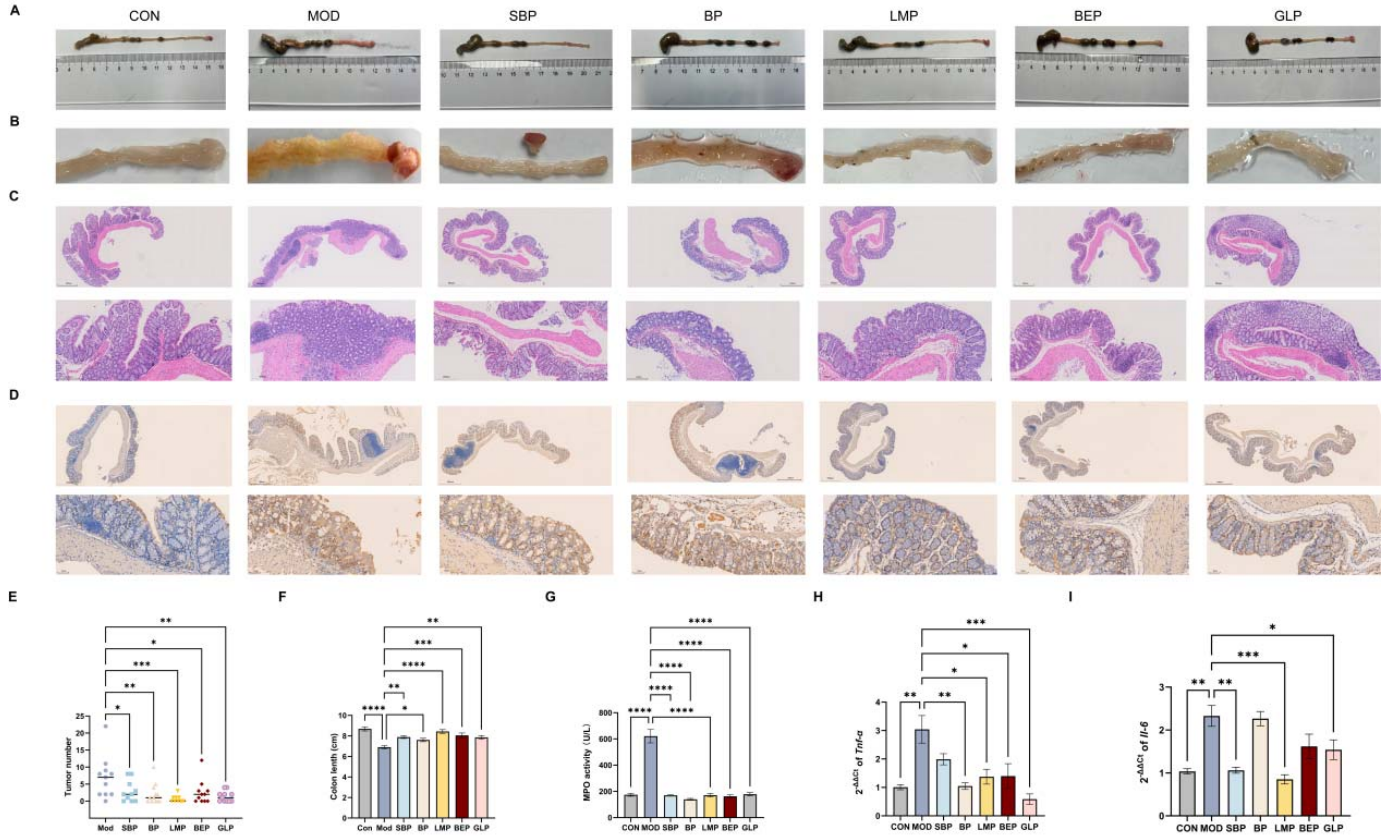

Fig. 2 Effect of BPs on AOM/DSS-induced colorectal cancer. (A) Representative images of colons and colon length in each group. (B) Representative gross images of colon tissues. (C) Representative H&E staining images of colon tissues (upper, low magnification; lower, high magnification). (D) Representative Ki67 immunohistochemical staining images of colon tissues (upper, low magnification; lower, high magnification). (E) Tumor number. (F) Colon length. (G) Serum MPO activity. (H) Relative mRNA expression of Tnf-α in colon tissues. (I) Relative mRNA expression of Il-6 in colon tissues. Data are expressed as mean ± SD. For qRT-PCR analysis of Tnf-α and Il-6, n = 3 per group. *$P < 0.05$, **$P < 0.01$, ***$P < 0.001$ by One-way ANOVA.

2.3 The mechanism of Lanmaoa asiatica polysaccharides in inhibiting colon cancer cells

2.3.1 Lanmaoa asiatica polysaccharides do not promote apoptosis in CRC Cells

Natural products can inhibit tumor cells through various pathways, commonly by inducing apoptosis or suppressing proliferation to halt tumor development. Annexin V-FITC/PI flow cytometry is frequently used to assess cellular apoptosis, where quadrant Q2 indicates late-stage apoptosis and quadrant Q4 represents early-stage apoptosis.

Apoptosis analysis showed that LMP did not induce apoptosis in HT-29 cells. This suggests that LMP may inhibit HT-29 colon cancer cells through other mechanisms (Fig. 3).

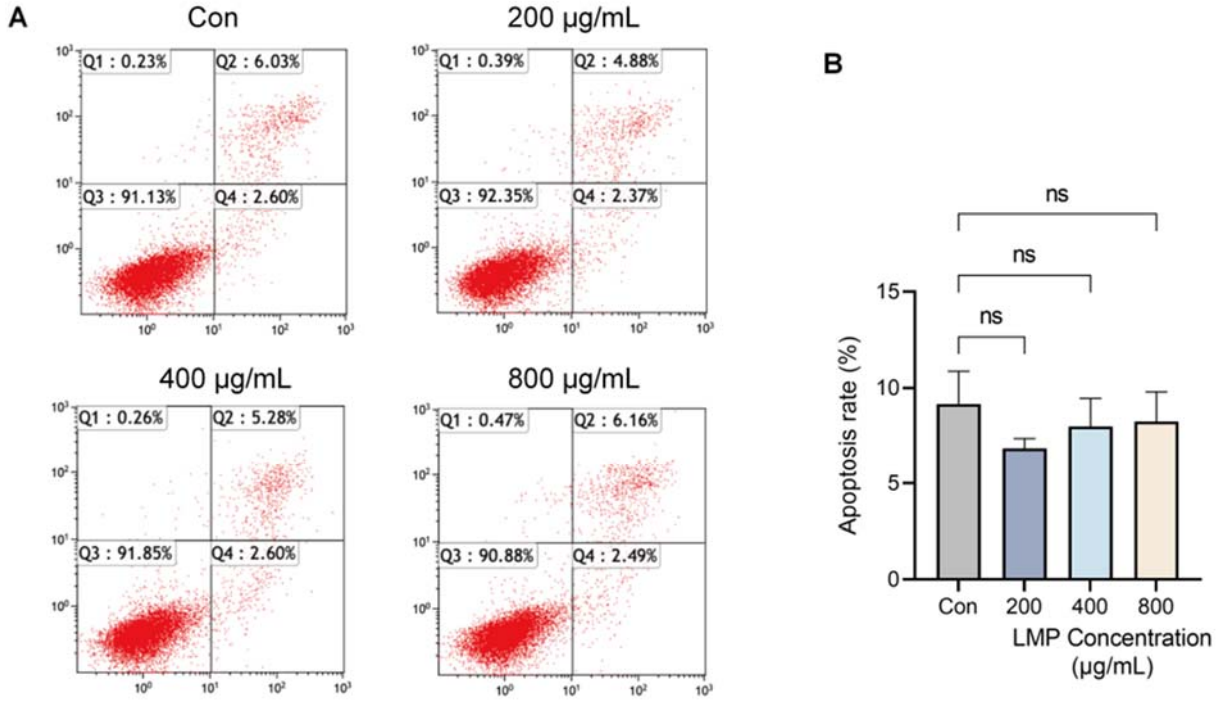

Fig. 3 Effects of LMP on apoptosis in HT-29 cells. HT-29 cells were treated with different concentrations of LMP (200, 400, and 800 μg/mL) for 24 h, and apoptosis was evaluated by Annexin V-FITC/PI double staining followed by flow cytometry. (A) Representative flow cytometry dot plots of different concentrations of LMP (0, 200, 400, and 800 μg/mL) . (B) The percentage of apoptotic cells (Q2 + Q4 quadrants). Data are expressed as mean ± SD (n =3). **P* < 0.05, ***P* < 0.01, ****P* < 0.001 by One-way ANOVA.

2.3.2 Inhibitory effect of Lanmaoa asiatica polysaccharides on CRC cell proliferation

The colony formation assay is commonly used to evaluate the proliferative capacity of cells, as only viable cells with sustained proliferative ability can form colonies. The results showed that LMP markedly inhibited colony formation in HT-29 cells, especially at concentrations of 400 and 800 μg/mL (Fig. 4A-B), suggesting that LMP suppresses the long-term proliferative potential of CRC cells. EdU incorporation assay further showed that LMP reduced DNA synthesis in HT-29 cells. The proportion of EdU-positive cells decreased significantly after LMP treatment, particularly at concentrations of 200 μg/mL and above (Fig. 4C-D), indicating that LMP inhibits cell proliferation. In addition, scratch wound-healing assay showed that LMP reduced the wound-healing rate of HT-29 cells, suggesting a suppressive effect on cell motility (Fig. 4E-F). Transwell assays further showed that LMP treatment decreased the numbers of migrated and invaded cells, with more obvious inhibition observed at higher concentrations (Fig. 4G–I). These findings indicate that, in addition to its antiproliferative activity, LMP also suppresses the migration- and invasion-related properties of HT-29 cells under the present experimental conditions.

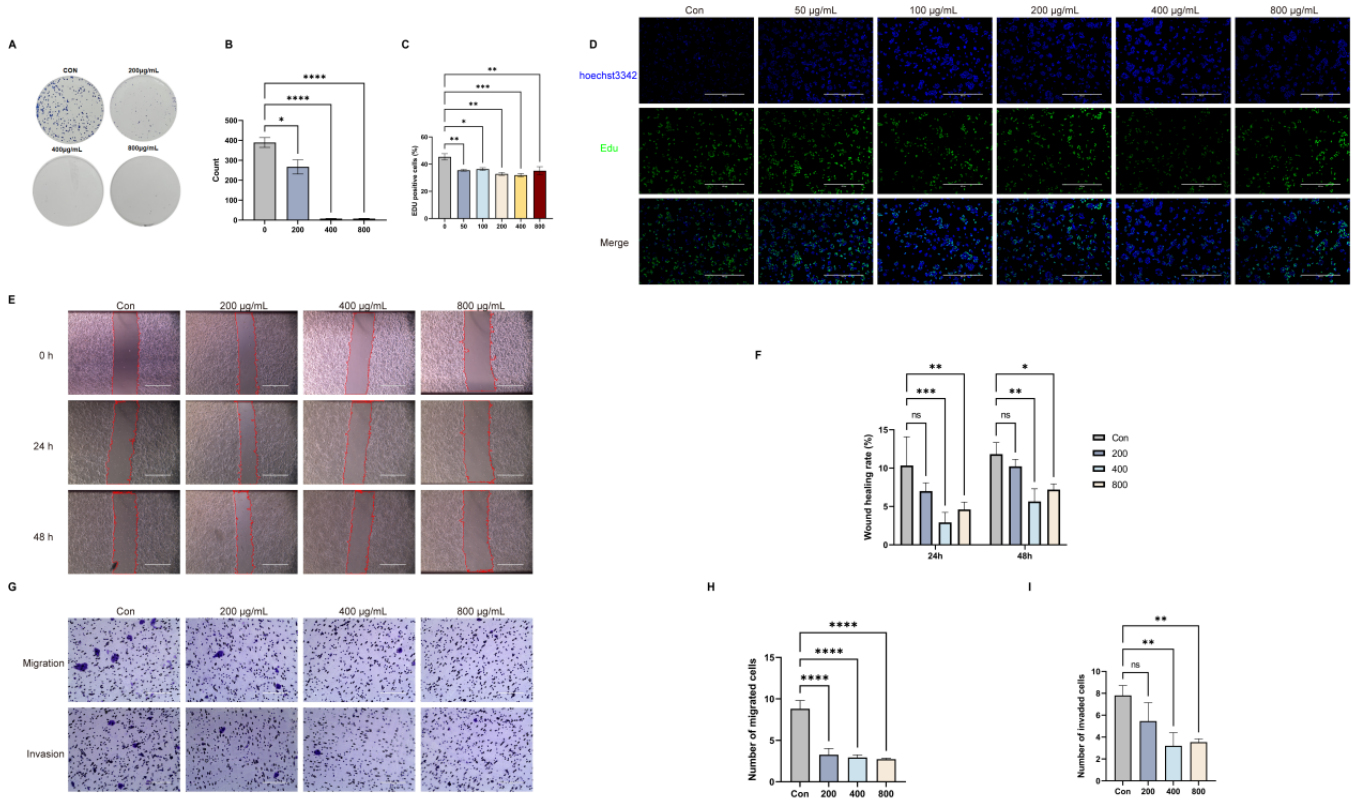

Fig. 4 LMP inhibited the proliferation and motility-related properties of HT-29 cells. (A) Representative images of colony formation in HT-29 cells treated with LMP (0, 200, 400, and 800 μg/mL). (B) Quantification of colony numbers. (C) Quantification of EdU-positive cells. (D) Representative fluorescence images of EdU incorporation (green) with Hoechst3342 nuclear staining (blue) in HT-29 cells treated with LMP (0, 50, 100, 200, 400, and 800 μg/mL) for 24 h. (E) Representative images of scratch wound-healing assays at 0, 24, and 48 h in HT-29 cells treated with LMP (0, 200, 400, and 800 μg/mL). (F) Quantification of wound-healing rate. (G) Representative images of Transwell migration and invasion assays in HT-29 cells treated with LMP (0, 200, 400, and 800 μg/mL). (H) Quantification of invaded cells. (I) Quantification of migrated cells. *$P < 0.05$, **$P < 0.01$, ***$P < 0.001$ by One-way ANOVA.

2.3.3 Effect of LMP on cell cycle progression in HT-29 cells

To investigate the mechanism by which LMP inhibits the proliferation of HT-29 cells, we analyzed the cell cycle distribution using flow cytometry. The results showed that, compared with the control group, LMP treatment (200, 400, and 800 μg/mL) led to a marked increase in the proportion of cells in the G1 phase, with a trend toward dose dependence. Correspondingly, the proportion of cells in the S phase decreased progressively, whereas the G2 phase proportion remained largely unchanged (Fig. 5). These findings suggest that LMP causes HT-29 cells to arrest in the G1 phase, thereby reducing their entry into the S phase for DNA synthesis.

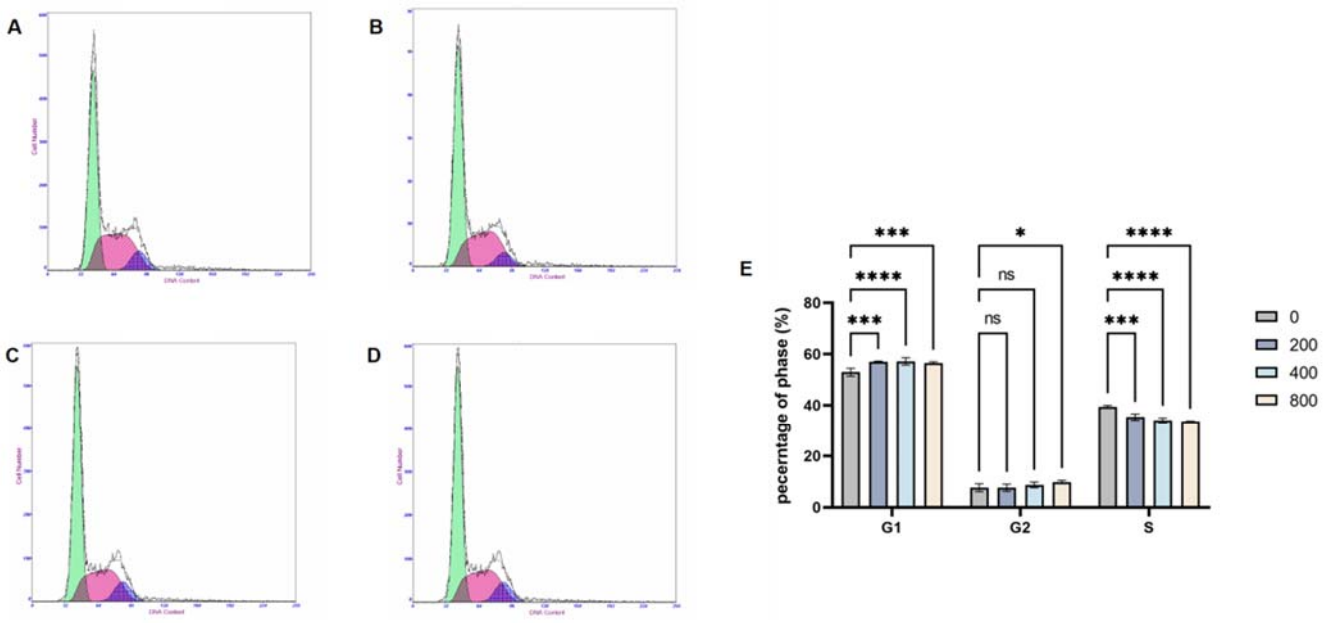

Fig. 5 Effects of LMP on the cell cycle distribution of HT-29 cells. HT-29 cells were treated with different concentrations of LMP (0, 200, 400, and 800 μg/mL) for 24 h, and cell cycle distribution was analyzed by flow cytometry with PI staining. (A-D) Representative histograms of different concentrations of LMP treatment (0, 200, 400, and 800 μg/mL). (E) The proportion of cells in G1, S, and G2/M phases. Data are expressed as mean ± SD (n =3). **P* < 0.05, ***P* < 0.01, ****P* < 0.001 by Two-way ANOVA.

2.3.4 Effects of LMP on cell cycle-related gene expression

To further investigate the molecular basis of the antiproliferative effect of LMP, we examined the expression of cell cycle-related genes *in vivo* and *in vitro*. In colon tissues, the mRNA expression levels of *Cdk2* and *Ccne1*, which are involved in the G1/S transition, were significantly increased in the model group compared with the control group, whereas LMP treatment reduced their expression (Fig. 6A–B).

In HT-29 cells, LMP treatment markedly downregulated the expression of *CDK2*, CCNE1, *SKP2,* and *PCNA* (Fig. 6C–E, G), while increasing the expression of *GADD45A* and *CDKN1A* (Fig. 6F, H). In addition, the expression levels of *H2AX* and *CHEK1* were also decreased after LMP treatment (Fig. 6I–J). These transcriptional changes were generally consistent with the flow cytometry results and suggest that LMP suppresses HT-29 cell proliferation at least in part by interfering with G1/S cell cycle progression.

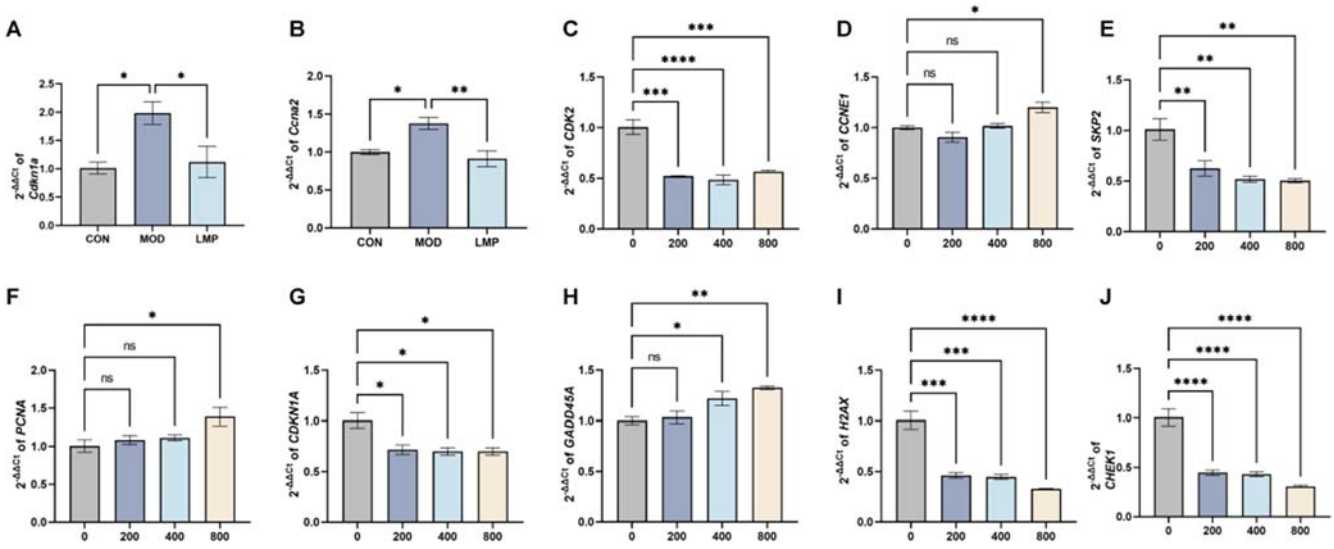

Fig. 6 Effects of LMP on cell cycle-related gene expression *in vivo* and in vitro. (A–B) Relative mRNA expression of *Cdk2* and *Ccne1* in colon tissues from control (CON), model (MOD), and LMP-treated (LMP) mice. (C–J) Relative mRNA expression of *CDK2*, *CCNE1*, *SKP2*, *GADD45A*, *PCNA*, *CDKN1A*, *H2AX*, and *CHEK1* in HT-29 cells treated with LMP (0, 200, 400, and 800 μg/mL) for 24 h, determined by qRT-PCR. Data are expressed as mean ± SD (n =3). **P* < 0.05, ***P* < 0.01, ****P* < 0.001 by One-way ANOVA.

Catalase (CAT), superoxide dismutase (SOD), and glutathione peroxidase (GSH-Px) are key antioxidant enzymes that protect cells from oxidative damage by scavenging reactive oxygen species (ROS) and limiting lipid peroxidation, whereas malondialdehyde (MDA) is a major end product of lipid peroxidation and reflects the extent of oxidative stress. After LMP treatment, the activities of CAT, SOD, and GSH-Px in HT-29 cells were significantly decreased (Fig. 7A–C), while the levels of MDA and ROS were markedly increased (Fig. 7D–E). The mRNA expression of *GPX4*, a key enzyme involved in detoxifying lipid peroxides, was significantly downregulated after LMP treatment (Fig. 7F). Western blot analysis further confirmed that GPX4 protein expression was decreased in HT-29 cells following LMP exposure (Fig. 7G–H). Consistently, immunofluorescence staining showed that GPX4 fluorescence intensity was markedly reduced in the LMP-treated group compared with the control group (Fig. 7I–J). These results indicate that LMP disrupts the antioxidant defense system and suppresses GPX4 expression, thereby promoting oxidative stress in HT-29 cells.

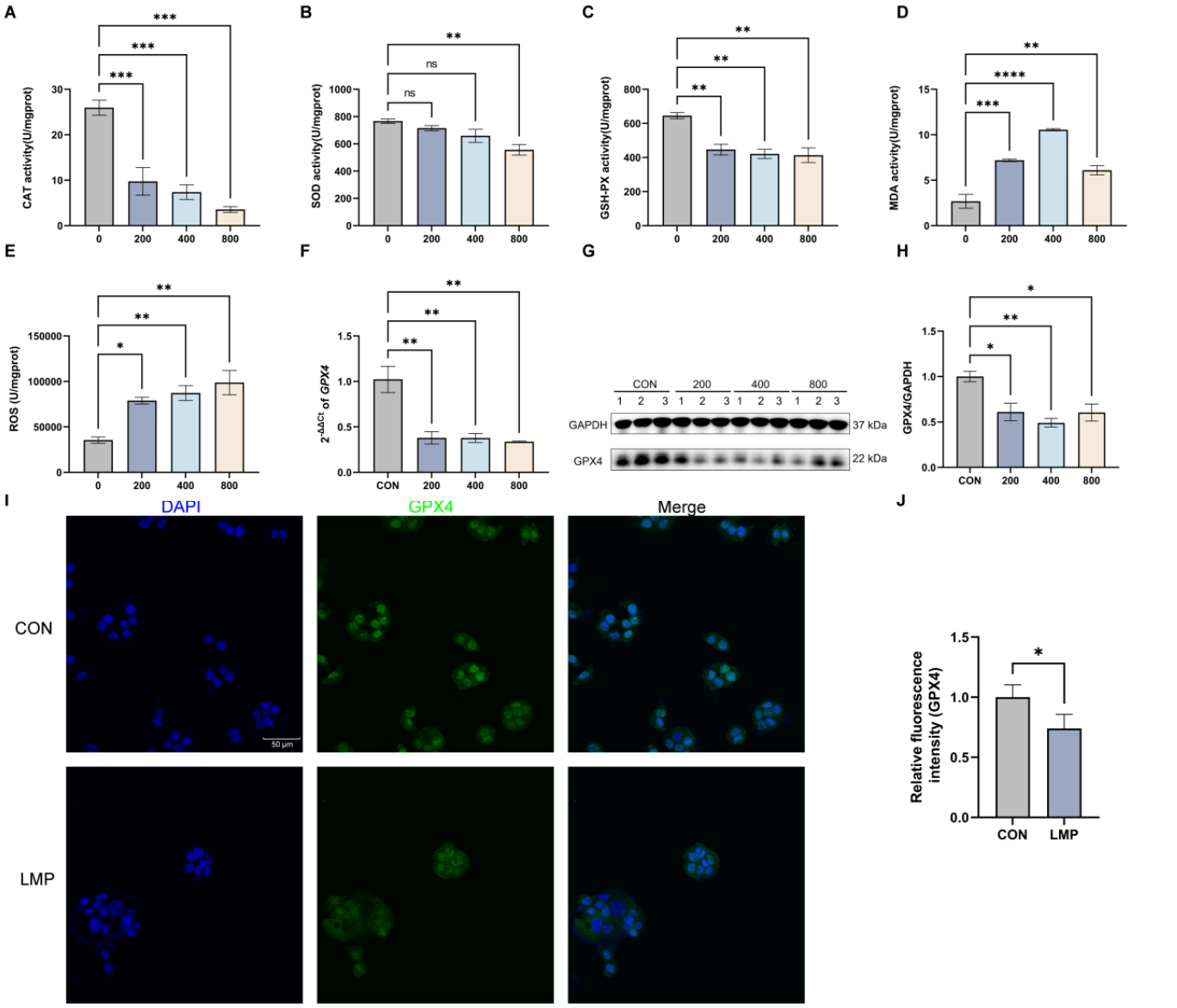

Fig. 7 Effects of LMP on oxidative stress and GPX4 expression in HT-29 cells. (A–C) Activities of CAT, SOD, and GSH-Px, respectively. (D–E) Levels of MDA and ROS, respectively. (F) Relative mRNA expression of *GPX4* determined by qRT-PCR. (G) Representative western blot images of GPX4 and GAPDH. (H) Quantification of GPX4 protein expression normalized to GAPDH. (I) Representative immunofluorescence images of GPX4 (green) with DAPI nuclear staining (blue) in control and LMP-treated HT-29 cells. (J) Quantification of relative fluorescence intensity of GPX4. Data are expressed as mean ± SD (n =3). **P* < 0.05, ***P* < 0.01, ****P* < 0.001 by One-way ANOVA.

We next examined the NRF2 signaling pathway. In colon tissues, Nrf2 expression was markedly elevated in the model group, whereas LMP treatment reduced its expression in vivo (Fig. 8A). A similar trend was observed in HT-29 cells, where LMP significantly decreased NRF2 mRNA levels in a dose-dependent manner (Fig. 8B). Immunofluorescence staining showed lower NRF2 fluorescence intensity after LMP treatment (Fig. 8C–D). Western blot analysis further showed that NRF2 protein expression was reduced in LMP-treated HT-29 cells (Fig. 8E–F).

As an important downstream target related to antioxidant responses, HO-1 was further examined. qRT-PCR results showed that *HO-1* mRNA expression was significantly decreased after LMP treatment (Fig. 8G). However, western blot analysis showed that HO-1 protein expression was increased (Fig. 8H–I). This

discordance between *HO-1* mRNA and HO-1 protein levels may reflect post-transcriptional or post-translational regulation under oxidative stress conditions.

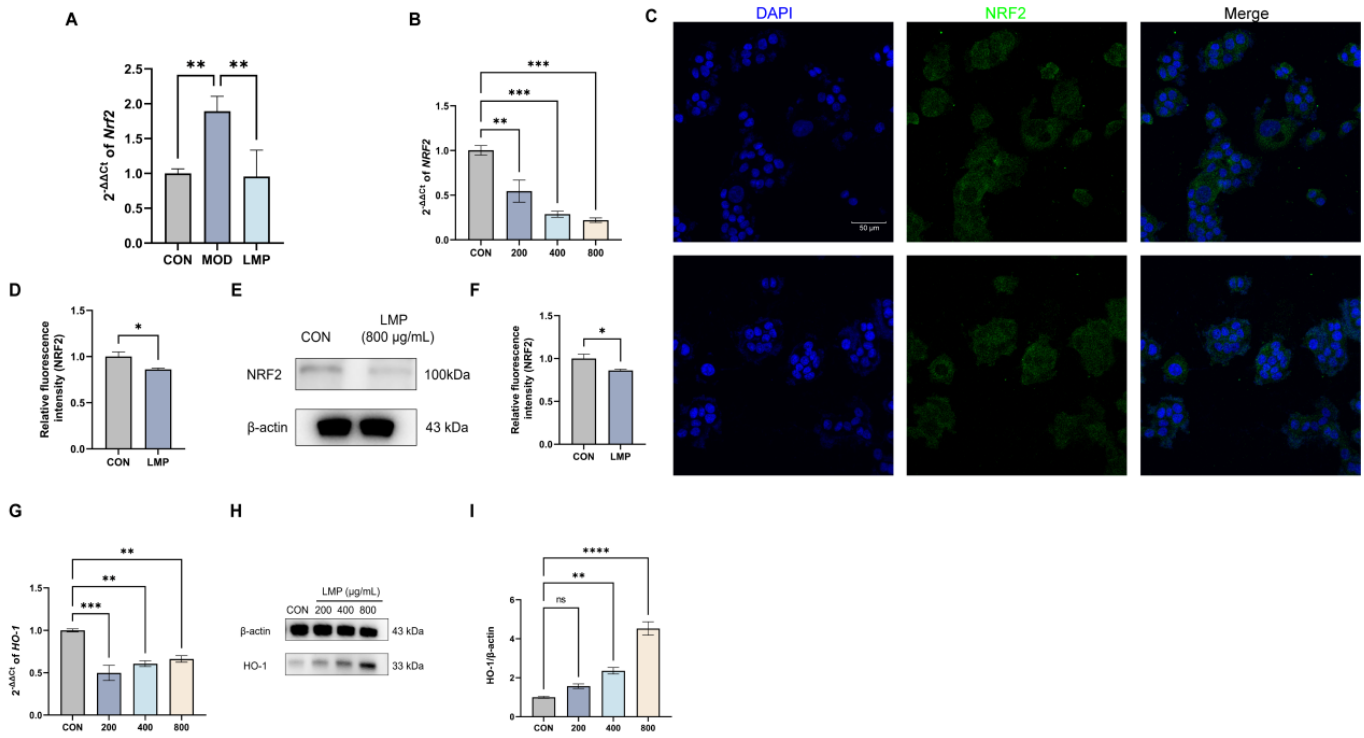

Fig. 8 Effects of LMP on NRF2/HO-1-related antioxidant signaling *in vivo* and *in vitro*. (A) Relative mRNA expression of *Nrf2* in colon tissues from control (CON), model (MOD), and LMP-treated (LMP) mice, determined by qRT-PCR. (B) Relative mRNA expression of *NRF2* in HT-29 cells treated with LMP (200, 400, and 800 μg/mL) for 24 h. (C) Representative immunofluorescence images of NRF2 (green) with DAPI nuclear staining (blue) in control and LMP-treated HT-29 cells. (D) Quantification of relative fluorescence intensity of NRF2. (E) Representative western blot images of NRF2 and β-actin in HT-29 cells. (F) Quantification of NRF2 protein expression normalized to β-actin. (G) Relative mRNA expression of *HO-1* in HT-29 cells treated with LMP (200, 400, and 800 μg/mL) for 24 h. (H) Representative western blot images of HO-1 and β-actin in HT-29 cells. (I) Quantification of HO-1 protein expression normalized to β-actin. Data are expressed as mean ± SD (n =3). **P* < 0.05, ***P* < 0.01, ****P* < 0.001 by One-way ANOVA.

3. Discussion

Edible boletes are widely distributed in southwestern China and parts of the Americas, with several species already used as edible fungi. Polysaccharides are the major bioactive constituents of Boletus, yet comparative studies on the anti-colorectal cancer (CRC) activities of different Boletus polysaccharides (BPs) remain limited. In this study, we evaluated and compared the antitumor effects of four bolete polysaccharides using both *in vitro* colorectal cancer cell lines and an *in vivo* AOM/DSS-induced CRC mouse model. All four polysaccharides exhibited varying degrees of antitumor activity, including suppression of tumor cell proliferation, reduction of tumor burden and colon length reduction, and alleviation of inflammation. Among them, *Lanmaoa asiatica* polysaccharide (LMP) exerted the most pronounced effects both *in vitro* and *in vivo*, and was therefore selected for mechanistic investigation.

Numerous studies have demonstrated that polysaccharides can directly suppress tumor cell growth *in vitro*. For example, *Ganoderma lucidum* polysaccharides inhibit proliferation and induce apoptosis in multiple cancer cell lines[18], and *Anacardium occidentale* polysaccharide suppresses HCT116 cell proliferation[19]. Consistently, our results showed that all tested BPs significantly inhibited the viability of CRC cell lines

HT-29 and CT26 without affecting normal colonic epithelial NCM460 cells, with LMP showing the strongest antiproliferative effect. *In vivo*, different types of polysaccharide gavage also displayed antitumor activity in CRC mouse models[20,21]. However, as most polysaccharides cannot be digested by gastrointestinal enzymes[22], the antitumor effects may involve gut microbiota–derived metabolites such as short-chain fatty acids (SCFAs), which are associated with reduced CRC risk[23]. To distinguish direct from microbiota-mediated effects, we established pseudo-germ-free CRC mice by administering antibiotics[24]. Our findings confirmed that BPs reduced tumor numbers even in pseudo-germ-free CRC mouse, suggesting that BPs may exert antitumor effects even under pseudo-germ-free conditions.

Chronic inflammation is a well-recognized driver of CRC initiation and progression[25]. Specifically, LMP treatment reduced MPO activity and inflammatory cytokines in AOM/DSS mice, indicating moderate anti-inflammatory effects. Nevertheless, further analyses suggested that the antiproliferative effect of LMP was more closely associated with redox imbalance and cell-cycle arrest than with inflammation suppression alone. Our findings suggest that LMP is associated with disturbed cellular redox homeostasis, accompanied by ROS accumulation, oxidative damage, and G1-phase arrest.

Consistent with flow cytometry results, LMP primarily suppressed CRC cells proliferation rather than inducing apoptosis, as confirmed by the reduced colony formation and DNA synthesis observed in EdU assays. These findings are consistent with previous reports that other polysaccharides, such as *hawthorn* and *Hericium erinaceus* polysaccharides, suppress CRC growth by inducing cell-cycle arrest[26,27]. LMP downregulated *CCNE1*, *CDK2*, *SKP2*, *H2AX* and *CHEK1*, while upregulating *GADD45A*, consistent with reports that Cyclin E1/CDK2 and SKP2 are essential for S-phase entry[28], whereas GADD45A mediates DNA damage responses and cell cycle arrest[29].

NRF2 is often aberrantly activated in tumors, promoting proliferation, survival, and chemoresistance[30]. In contrast, LMP treatment markedly downregulated *NRF2* expression at the mRNA level, accompanied by decreased activities of downstream antioxidant enzymes (SOD, CAT, GSH-Px). Reduced NRF2 expression, together with decreased antioxidant enzyme activities, was associated with impaired antioxidant defense and ROS accumulation. The elevated ROS can activate ATM/Chk1/Chk2 signaling and trigger cell cycle arrest, thereby contributing to the inhibition of tumor cell proliferation[31]. Increased oxidative stress may contribute to DNA damage responses and cell-cycle arrest. GPX4, a key enzyme in lipid peroxide detoxification, was also decreased. GPX4 depletion has been reported to cause G0/G1 arrest and inhibit tumor proliferation[32]. GPX4 downregulation may also participate in this process by weakening lipid peroxide detoxification.

Interestingly, HO-1 protein expression was increased despite reduced mRNA levels, suggesting possible post-transcriptional or post-translational regulation. Previous studies have shown that oxidative stress can increase HO-1 protein abundance without a corresponding increase in mRNA, partly through deubiquitination- and stabilization-related mechanisms[33]. Therefore, one possible explanation is that LMP-induced oxidative stress may promote HO-1 protein stabilization, leading to discordant HO-1 mRNA and protein expression. Because the present study did not directly investigate the regulatory mechanism or

functional contribution of HO-1, the precise role of HO-1 in the antiproliferative effect of LMP remains to be clarified. Nevertheless, previous studies have reported that HO-1 upregulation can be associated with suppressed proliferation, cell-cycle arrest, and reduced tumor burden in colorectal or breast cancer models[34,35].

Collectively, these findings suggest that LMP suppresses colorectal tumor cell growth in association with NRF2–GPX4-related redox imbalance. These changes are accompanied by DNA damage responses and G1-phase arrest, while elevated HO-1 levels may further enhance ROS accumulation and impair antioxidant defenses, reinforcing cell-cycle blockade. These results provide new insight into the redox-related antitumor mechanisms of bolete polysaccharides and support their potential as functional food ingredients for colorectal cancer prevention.

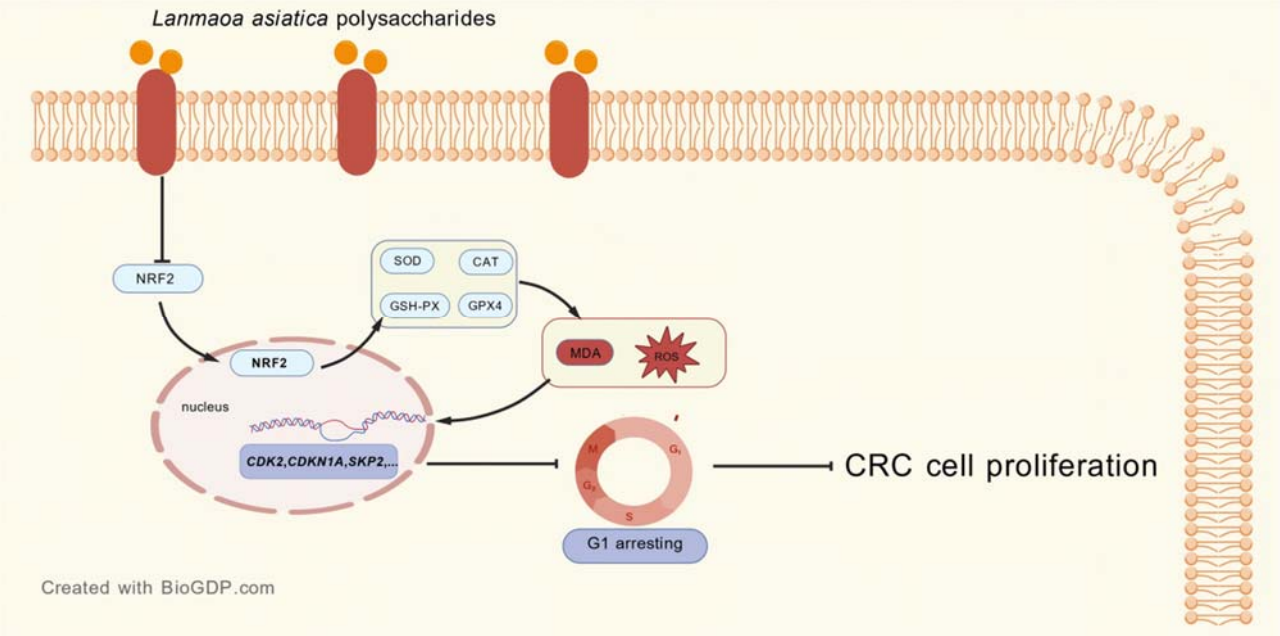

Fig. 9 Proposed redox-related mechanism of LMP in suppressing colorectal cancer cell proliferation. LMP may inhibit CRC cell growth through redox imbalance associated with reduced NRF2 and GPX4 expression, ROS accumulation, oxidative damage, and G1-phase cell-cycle arrest. Schematic diagram was created with BioGDP.com[36].

4. Methods

4.1 Reagents and materials

Suillus bovinus (SBP), *Boletus* sp. closely related to *B. recapitulatus* (BP), *Lanmaoa asiatica* (LMP), and *Boletus* sp. closely related to *B. edulis* (BEP) were purchased from Yunnan, China (Dianfeng Junye Wild Mushroom). The mushroom materials were assigned based on ITS sequence analysis and comparison with reference sequences in GenBank. NCM460, CT26, and HT-29 cell lines; McCoy's 5a medium; and fetal bovine serum (FBS) were obtained from Pricella Biotechnology Co., Ltd. (Wuhan, China).RPMI-1640 medium, high-glucose Dulbecco's Modified Eagle Medium (DMEM), and penicillin-streptomycin were purchased from Gibco™, Thermo Fisher Scientific, (Waltham, MA, USA).The Cell Counting Kit-8 (CCK-8) was purchased from GLPBIO Technology Inc. (Montclair, CA, USA). TransZol Up kit was obtained from TransGen Biotech (Beijing, China). The RNA extraction kit, HiScript IV All-in-one Ultra RT SuperMix, and

ChamQ Universal SYBR qRT-PCR Master Mix were purchased from Vazyme Biotech Co., Ltd. (Nanjing, China). Edu assay kit, Modified Giemsa Staining Solution and BCA protein assay kit were purchased from Beyotime Biotechnology (Shanghai, China). The **myeloperoxidase** (MPO) assay kits were purchased from Jiancheng Bioengineering Co., Ltd. (Nanjing, China). Annexin V-FITC/PI Apoptosis Detection Kit (Cat. No. 556547) and PI were purchased from Becton, Dickinson and Company (BD, Franklin Lakes, NJ, USA). Azoxymethane was purchased from Sigma-Aldrich (Darmstadt, Germany).Dextran sulfate sodium (DSS) was purchased from MP Biomedicals(Santa Ana, CA, USA). All other chemicals and reagents used in this study were of analytical grade.

4.2 Preparation of polysaccharides

The dried fruiting bodies of the selected boletes were ground into powder and defatted by soaking in 90% ethanol overnight. The defatted powder was then subjected to hot water extraction three times at a solid-to-liquid ratio of 1:30 (w/v), with each extraction lasting 120 min. The combined extracts were treated with 1% neutral protease (w/v) for 4 hours at 50 °C. Subsequently, proteins were removed from the polysaccharide solution using the Sevag method. Residual organic solvents were then removed using a rotary vacuum evaporator. Anhydrous ethanol was added to the solution at a ratio of 4:1 (v/v) to the polysaccharide solution volume, and the mixture was left overnight at 4 °C to precipitate the crude polysaccharides. The precipitate was redissolved in distilled water and dialyzed against a 3,500 Da molecular weight cut-off dialysis bag for 48 hours. Finally, the crude polysaccharide samples from the corresponding bolete materials were obtained by lyophilization.

4.3 Cell culture and assays

4.3.1 Cell viability assay

Resuscitated NCM460, CT26, and HT-29 cells were cultured in their respective basal media (DMEM high glucose, RPMI-1640, or McCoy's 5a) supplemented with 10% FBS and 1% penicillin-streptomycin at 37 °C in a 5% CO_2 incubator. Different BPs were diluted in culture medium and sterilized by filtration for subsequent experiments. A cell suspension of 8,000 cells per well was seeded into 96-well plates. After 24 h, the medium was removed and replaced with 100 μL of fresh medium containing BPs at various concentrations (0, 25, 50, 100, 200, 400, 800, 1600 μg/mL). The cells were cultured for another 24 h. After the medium was removed, 10% CCK8 reagent was added to each well. The plates were incubated for 2 h, and the absorbance was measured at 450 nm. Cell viability was calculated relative to the 0 μg/mL concentration group.

4.3.2 Cell colony formation assay

HT-29 cells were seeded into 6-well plates at a density of 1,000 cells per well. After 24 h, the medium was replaced with fresh medium containing different concentrations of LMP (0, 200, 400, 800 μg/mL). The cells were cultured for 10–14 days, with the medium being refreshed every 3 days. At the end of the incubation period, the medium was discarded, and the colonies were gently washed with PBS. The cells were then fixed with 4% paraformaldehyde, stained with modified Giemsa staining solution, and photographed.

4.3.3 EdU cell proliferation assay

HT-29 cells were seeded into 12-well plates at a density of 2 × 10^5 cells per well. After 24 h, the cells were treated with different concentrations of LMP (0, 200, 400, 800 μg/mL) for 24 h. After treatment, EdU was added to each well at a final concentration of 10 μM, and the cells were incubated for another 2 h. Cells were then fixed with 4% paraformaldehyde. After fixation, the cells were washed with a washing buffer (PBS containing 3% BSA) and permeabilized with 0.3% Triton X-100 in PBS. The Click reaction mixture was added and incubated for 30 min, followed by three washes. The cell nuclei were stained with 1X Hoechst 33342. Images were captured using a cell imaging system at 488 nm and 495 nm channels.

4.3.4 Wound healing assay

Cells were seeded in 6-well plates at a density of 1.2×10^6 cells per well. Once the cell confluence reached approximately 90%, a linear scratch was created using a sterile pipette tip. The cell debris was removed by washing with PBS. Subsequently, the cells were incubated with serum-free medium containing various concentrations of LMP (0, 200, 400, and 800 μg/mL). The initial wound areas were photographed immediately after scratching (0 h). After 24 h and 48 h of incubation, the wound closure was observed and captured using an inverted microscope.

4.3.5 Cell migration and invasion assays

Cell migration and invasion were evaluated using Transwell chambers. For the invasion assay, the upper chamber was pre-coated with diluted Matrigel (1:9) and incubated until a gel layer formed. Treated cells (1.0×10^5 cells/well) were resuspended in serum-free medium and added to the upper chamber, while medium containing 20% FBS was added to the lower chamber as a chemoattractant.After an appropriate incubation period, the cells that had successfully moved to the lower surface of the membrane were fixed with 4% paraformaldehyde and stained with crystal violet. The migration and invasion capacities were quantified by counting the stained cells in several randomly selected fields under a microscope. Each experiment was conducted in triplicate.

4.3.6 Cell apoptosis assay

HT-29 cells were seeded into 6-well plates at a density of 5 × 10^5 cells per well. After 24 h, the cells were treated with different concentrations of LMP (0, 200, 400, 800 μg/mL) for 24 h. After treatment, both adherent and floating cells were collected using a cell scraper (without EDTA) and washed with PBS. After centrifugation, the supernatant was discarded, and the cell pellet was resuspended in 100 μL of Binding Buffer. After mixing, 2.5 μL Annexin V-FITC and 2.5 μL PI were added. The cells were incubated in the dark for 15 min. After adding 200 μL of Binding Buffer, apoptosis was detected using a flow cytometer. The flow cytometer used a 488 nm excitation laser for detection. FlowJo software was used to analyze the data and generate dot plots of FITC-A vs. PI-A, distinguishing between early apoptotic (ANNEXIN V^+/PI^-), late apoptotic (ANNEXIN V^+/PI^+), necrotic (ANNEXIN V^-/PI^+), and live (ANNEXIN V^-/PI^-) cell populations.

4.3.7 Cell cycle assay

Cell culture and LMP treatment methods were the same as those described in Section 2.3.4. After collection, the cells were washed with PBS, the supernatant was discarded, and the cells were fixed in 70% ethanol overnight at 4 °C. After centrifugation to remove the ethanol and a single wash with PBS, the cells were stained with a PI solution containing RNase for 15 min. Cell cycle distribution was then analyzed using a flow cytometer. The flow cytometer was set to an excitation wavelength of 488 nm and an emission fluorescence detection filter range of 510–530 nm.

4.3.8 Determination of antioxidant enzyme activity and MDA levels

Cell culture and drug administration methods were the same as those described in Section 2.3.5. The protein content of supernatants from each group was determined using a BCA kit, following the manufacturer's instructions. The the levels of relevant antioxidant enzymes (SOD, CAT, GSH-PX) and oxidative stress marker (MDA) were determined using detection kits following the manufacturer's instructions. The final results were based on the total amount of protein measured in each group.

4.3.9 Determination of ROS level

Cell culture and drug administration methods were the same as those described in Section 2.3.1. After 24 h treatment, the culture medium was removed, and the cells were washed twice with serum-free medium. DCFH-DA was added at a final concentration of 10 μM, followed by incubation at 37 °C in the dark for 30 min. After incubation, the DCFH-DA solution was discarded, and the cells were washed twice with PBS. The fluorescence intensity of each well was immediately measured using a microplate reader at an excitation wavelength of 488 nm and an emission wavelength of 525 nm.

4.4 Animal experiments

4.4.1 Animal housing

All animal experiments were performed with the approval of the Ethics Committee for Animal Experimentation of Jinan University (Ethical Approval No.: 20240913-07) and strictly adhered to all guidelines regarding the care and use of laboratory animals. The experimental design aimed to minimize the number of animals and their suffering. A total of 84 male SPF-grade BALB/c mice (6-8 weeks old, 20 g) were purchased from Vital River Laboratory Animal Technology Co., Ltd. The mice were housed at the Experimental Animal Management Center of Jinan University School of Medicine under controlled conditions (temperature 23 ± 2 °C, humidity 55% ± 5%, and a 12 h light/12 h dark cycle). Mice had free access to food and water throughout the experiment and were fed an AIN-93M standard diet. After a 10-day acclimation period, subsequent experiments were conducted. The experiment concluded 19 weeks after the AOM injection, at which point the mice were euthanized with with 400 μL 1.25% 2,2,2-tribromoethanol per mouse by intraperitoneal injection. The absence of reflexes (such as the pedal and corneal reflexes) confirmed that the mice were fully anesthetized. Following deep anesthesia, blood was collected from the retro-orbital plexus, centrifuged at 3000 × g for 10 minutes, and the resulting serum was separated and stored at −80 °C. Subsequently, the mice were euthanized by cervical dislocation. The entire colon was carefully removed, and

its length and the number of tumors were recorded. Mouse serum, colon tissue, heart, liver, kidneys, and spleen were collected and stored at -80 °C for further analysis. All experimental procedures were conducted in strict accordance with institutional ethical standards and were approved by the Institutional Animal Care and Use Committee (IACUC).

4.4.2 Establishment of the AOM/DSS-induced CRC and pseudo-germ-free animal models

After the acclimation period, mice were randomly divided into groups of 12: Control (Con), Model (Mod), *Suillus bovinus* polysaccharide (SBP), *Boletus recapitulatus* polysaccharide (B), *Lanmaoa asiatica* polysaccharide (LMP), *Boletus bainiugan* polysaccharide (BEP) and *Ganoderma lucidum* polysaccharide (GLP) groups. Except for the Control group, all mice received an intraperitoneal injection of AOM (10 mg/kg) on Day 0 of the experiment. On Day 8 to Day 12, Day 29 to Day 33, Day 50 to Day 54, Day 70 to Day 74, the drinking water was replaced with 2.5% DSS to establish the CRC model. On Day 1 to Day 7, Day 14 to Day 21, Day 40 to Day 47, Day 56 to Day 63, Day 76-83, the drinking water was replaced with a mixed antibiotic solution (vancomycin 0.5 g/L, ampicillin 1 g/L, neomycin 1 g/L, and metronidazole 1 g/L). All groups drank sterile water on the remaining days. Starting from Day 1, mice in the SBP, B, LMP, BEP, and GLP groups received daily oral gavage of their respective polysaccharides at 300 mg/kg until the end of the experiment. The other groups were gavaged with sterile water. The experiment lasted for 90 days. This broad-spectrum antibiotic combination has been shown in multiple studies to significantly reduce the abundance of intestinal flora in mice[37,38] This study used the same treatment regimen to minimize the interference of intestinal flora on the effects of polysaccharides.

4.4.3 H&E staining

The collected colon tissues were fixed in 4% paraformaldehyde, dehydrated, and embedded in paraffin. Tissue sections were then stained with hematoxylin-eosin (H&E) to evaluate histological changes. For immunohistochemistry (IHC), sections were subjected to heat-induced antigen retrieval and incubated with anti-Ki67 primary antibody (1:1000; Cell Signaling Technology, #12202) overnight at 4°C. The signal was detected using an HRP-conjugated secondary antibody and visualized with DAB, followed by hematoxylin counterstaining.

4.4.4 Myeloperoxidase (MPO) activity

Serum MPO levels were measured according to the manufacturer's instructions.

4.5 Real-time Quantitative PCR (RT-qRT-PCR)

In the animal experiments, total RNA was extracted from mouse colon tissues using TRIzol reagent. For HT-29 cells, total RNA was extracted using a commercial RNA extraction kit after being cultured in the same manner as described in Section 4.3.3. The RNA concentration was determined using a NanoDrop 2000 spectrophotometer. Following the manufacturer's instructions, RNA was reverse-transcribed into cDNA using the HiScript IV All-in-one Ultra RT SuperMix kit. RT-qRT-PCR was performed on the cDNA using the ChamQ Universal SYBR qRT-PCR Master Mix. *GAPDH* was used as an internal reference gene for

normalization, and relative gene expression was calculated using the $2^{-\Delta\Delta CT}$ method. The primers used in this study are listed in Table S1-2 and were designed by Sangon Biotech Co., Ltd. (Shanghai, China).

4.6 Western blotting

Western blotting was performed to assess protein expression levels. Colon tissue and cell samples were lysed in RIPA buffer and centrifuged at 15,000 × g for 15 min at 4 °C. The resulting supernatant was collected, and protein concentrations were determined using a BCA assay. Equal amounts of protein were separated by SDS-PAGE and transferred onto PVDF membranes. The membranes were blocked with 5% skim milk in TBST for 2 h at room temperature and then incubated with primary antibodies overnight at 4 °C. The following primary antibodies were used: anti-GPX4 (1:1,000; Abcam, Cambridge, UK, ab125066), anti-NRF2 (1:1000;Cell Signaling Technology, Danvers, MA, USA;,12721), anti-HO-1 (1:5000; Proteintech, Wuhan, Hubei, China, 10701-1-AP), anti-β-actin (1:5000; Proteintech, Wuhan, Hubei, China, 81115-1-RR) and anti-GAPDH (1:10,000; Proteintech, Wuhan, Hubei, China, 60004-1-Ig). After three washes with TBST (10 min each), membranes were incubated with HRP-conjugated secondary antibody (1:10,000; APExBIO, Houston, USA, K1223) for 2 h at room temperature. Protein signals were detected using ECL luminescent reagent (3–5 min; P10100, NCM Biotech Co., Ltd., Suzhou, China), and band intensities were quantified using grayscale analysis. Original blots is shown in Fig. S1.

4.7 Immunofluorescence Staining

The expression and subcellular localization of NRF2 and GPX4 were detected by immunofluorescence. Briefly, HT-29 cells in the control and 800 μg/mL LMP-treated groups were fixed with 4% paraformaldehyde and permeabilized with 0.5% Triton X-100, followed by blocking with 5% BSA for 1 h. The cells were then incubated with primary antibodies against NRF2 or GPX4 at 4°C overnight. After washing, the cells were incubated with Alexa Fluor 488-conjugated secondary antibodies for 1 h in the dark. Nuclei were counterstained with DAPI, and the fluorescent signals were observed and captured using a fluorescence microscope.

4.8 Statistical analysis

All data are expressed as the mean ± standard deviation (SD). Statistical analysis and graphing were performed using GraphPad Prism 9.5 software. Differences between groups were analyzed using a one-way analysis of variance (ANOVA) or an unpaired t-test. A p-value less than 0.05 was considered to be statistically significant.

Conclusion

Against this background, *Lanmaoa asiatica* polysaccharide (LMP) exerts dual effects: alleviating inflammation and downregulating antioxidant factors NRF2 and GPX4 in tumor cells, which may contribute to cell cycle arrest and the subsequent suppression of CRC cell proliferation (Fig. 9). Compared with healthy individuals, CRC patients typically present with dysbiosis, characterized by reduced probiotics and increased

pathogenic bacteria[39]. These findings suggest that LMP may have potential clinical significance in CRC patients during gut microbiota restoration.

Conflict of interest

The authors declared that they have no conflict of interest.

Acknowledgements

The authors thank Xinqiang Lai from Analytical and Testing Center of Jinan University for instructions on flow cytometry analysis.

Funding

This study was conducted with the internal resources of the research team and received no external funding.

Data availability

All data included in this study are available upon request.

Reference

[1] Colorectal cancer, (n.d.). https://www.who.int/news-room/fact-sheets/detail/colorectal-cancer (accessed July 23, 2025).

[2] G. Mauri, G. Patelli, G. Crisafulli, S. Siena, A. Bardelli, Tumor "age" in early-onset colorectal cancer, Cell 188 (2025) 589–593. https://doi.org/10.1016/j.cell.2024.12.003.

[3] Z. Zhou, L. Kleis, A. Depetris-Chauvin, S. Jaskulski, V. Damerell, K.B. Michels, B. Gigic, U. Nöthlings, G. Panagiotou, Beneficial microbiome and diet interplay in early-onset colorectal cancer, EMBO Mol. Med. 17 (2024) 9–30. https://doi.org/10.1038/s44321-024-00177-0.

[4] N. Akimoto, T. Ugai, R. Zhong, T. Hamada, K. Fujiyoshi, M. Giannakis, K. Wu, Y. Cao, K. Ng, S. Ogino, Rising incidence of early-onset colorectal cancer: a call for action, Nat. Rev. Clin. Oncol. 18 (2021) 230–243. https://doi.org/10.1038/s41571-020-00445-1.

[5] S.K. Veettil, T.Y. Wong, Y.S. Loo, M.C. Playdon, N.M. Lai, E.L. Giovannucci, N. Chaiyakunapruk, Role of Diet in Colorectal Cancer Incidence, JAMA Netw. Open 4 (2021) e2037341. https://doi.org/10.1001/jamanetworkopen.2020.37341.

[6] Y.-J. Wang, Q.-M. Li, X.-Q. Zha, J.-P. Luo, Intervention and potential mechanism of non-starch polysaccharides from natural resources on ulcerative colitis: A review, Int. J. Biol. Macromol. 210 (2022) 545–564. https://doi.org/10.1016/j.ijbiomac.2022.04.208.

[7] D. Liao, C. Cheng, J. Liu, L. Zhao, D.-C. Huang, G. Chen, Characterization and antitumor activities of polysaccharides obtained from ginger (*Zingiber officinale*) by different extraction methods, Int. J. Biol. Macromol. 152 (2020) 894–903. https://doi.org/10.1016/j.ijbiomac.2020.02.325.

[8] X. Hou, J. Liu, Z. Li, M. Chang, M. Guo, C. Feng, J. Shi, Fruiting body polysaccharides of Hericium erinaceus induce apoptosis in human colorectal cancer cells via ROS generation mediating caspase-9-dependent signaling pathways, Food Funct. 11 (2020) 6128–6138. https://doi.org/10.1039/D0FO00916D.

[9] C. Guo, D. Guo, L. Fang, T. Sang, J. Wu, C. Guo, Y. Wang, Y. Wang, C. Chen, J. Chen, R. Chen, X. Wang, Ganoderma lucidum polysaccharide modulates gut microbiota and immune cell function to inhibit inflammation and tumorigenesis in colon, Carbohydr. Polym. 267 (2021) 118231. https://doi.org/10.1016/j.carbpol.2021.118231.

[10] M. Ho Do, Y.S. Seo, H.-Y. Park, Polysaccharides: bowel health and gut microbiota, Crit. Rev. Food Sci. Nutr. 61 (2021) 1212–1224. https://doi.org/10.1080/10408398.2020.1755949.

[11] G. van Weelden, M. Bobiński, K. Okła, W.J. van Weelden, A. Romano, J.M.A. Pijnenborg, Fucoidan Structure and Activity in Relation to Anti-Cancer Mechanisms, Mar. Drugs 17 (2019) 32. https://doi.org/10.3390/md17010032.

[12] I.A. Schepetkin, M.T. Quinn, Botanical polysaccharides: macrophage immunomodulation and therapeutic potential, Int. Immunopharmacol. 6 (2006) 317–333. https://doi.org/10.1016/j.intimp.2005.10.005.

[13] Y. Tan, N.-K. Zeng, B. Xu, Chemical profiles and health-promoting effects of porcini mushroom (Boletus edulis): A narrative review, Food Chem. 390 (2022) 133199. https://doi.org/10.1016/j.foodchem.2022.133199.

[14] T. Meng, S. Yu, H. Ji, X. Xu, A. Liu, A novel acid polysaccharide from Boletus edulis: extraction, characteristics and antitumor activities in vitro, Glycoconj. J. 38 (2021) 13–24. https://doi.org/10.1007/s10719-021-09972-0.

[15] M.K. Lemieszek, C. Cardoso, F.H.F.M. Nunes, A.I.R.N.A. de Barros, G. Marques, P. Pożarowski, W. Rzeski, Boletus edulis biologically active biopolymers induce cell cycle arrest in human colon adenocarcinoma cells, Food Funct. 4 (2013) 575–585. https://doi.org/10.1039/C2FO30324H.

[16] Z. Li, S. Fan, X. Wang, L. Wang, J. Lv, J. Zhang, Extraction Optimization and Characterization of Antioxidant Polysaccharides From Suillus bovinus, Food Sci. Nutr. 13 (2025) e70995. https://doi.org/10.1002/fsn3.70995.

[17] D. Wang, S.-Q. Sun, W.-Z. Wu, S.-L. Yang, J.-M. Tan, Characterization of a water-soluble polysaccharide from boletus edulis and its antitumor and immunomodulatory activities on renal cancer in mice, Carbohydr. Polym. 105 (2014) 127–134. https://doi.org/10.1016/j.carbpol.2013.12.085.

[18] L. Fang, Q. Zhao, C. Guo, D. Guo, Z. Li, J. Xu, C. Guo, T. Sang, Y. Wang, J. Chen, C. Chen, R. Chen, J. Wu, X. Wang, Removing the sporoderm from the sporoderm-broken spores of Ganoderma lucidum improves the anticancer and immune-regulatory activity of the water-soluble polysaccharide, Front. Nutr. 9 (2022) 1006127. https://doi.org/10.3389/fnut.2022.1006127.

[19] F. de Oliveira Silva Ribeiro, F. de França Dourado, M.F.S. Silva, L.M. Brito, C. Pessoa, L.R.M. de Lima, R.C.M. de Paula, J.R. de Souza de Almeida Leite, A.R. de Araújo, D.A. da Silva, Anti-proliferative profile of *Anacardium occidentale* polysaccharide and characterization by AFM, Int. J. Biol. Macromol. 156 (2020) 981–987. https://doi.org/10.1016/j.ijbiomac.2020.03.145.

[20] Q. Li, C. Zhang, G. Xu, X. Shang, X. Nan, Y. Li, J. Liu, Y. Hong, Q. Wang, G. Peng, Astragalus polysaccharide ameliorates CD8+ T cell dysfunction through STAT3/Gal-3/LAG3 pathway in inflammation-induced colorectal cancer, Biomed. Pharmacother. Biomedecine Pharmacother. 171 (2024) 116172. https://doi.org/10.1016/j.biopha.2024.116172.

[21] Q. Wang, Y. Huang, M. Jia, D. Lu, H.-W. Zhang, D. Huang, S.-H. Liu, C. Lv, Safflower Polysaccharide Inhibits AOM/DSS-Induced Mice Colorectal Cancer Through the Regulation of Macrophage Polarization, Front. Pharmacol. 12 (2021) 761641. https://doi.org/10.3389/fphar.2021.761641.

[22] G. Ma, H. Du, Q. Hu, W. Yang, F. Pei, H. Xiao, Health benefits of edible mushroom polysaccharides and associated gut microbiota regulation, Crit. Rev. Food Sci. Nutr. 62 (2021) 6646–6663. https://doi.org/10.1080/10408398.2021.1903385.

[23] S.D. Gomes, C.S. Oliveira, J. Azevedo-Silva, M.R. Casanova, J. Barreto, H. Pereira, S.R. Chaves, L.R. Rodrigues, M. Casal, M. Côrte-Real, F. Baltazar, A. Preto, The Role of Diet Related Short-Chain Fatty Acids in Colorectal Cancer Metabolism and Survival: Prevention and Therapeutic Implications, Curr. Med. Chem. 27 (2020) 4087–4108. https://doi.org/10.2174/0929867325666180530102050.

[24] J. Luo, Q. Yang, W. Jiang, Y. Liu, Q. Hu, X. Peng, The interaction between *Angelica sinensis* polysaccharide ASP-2pb and specific gut bacteria alleviates rheumatoid arthritis in rats, Int. J. Biol. Macromol. 301 (2025) 140473. https://doi.org/10.1016/j.ijbiomac.2025.140473.

[25] M. Lucafò, D. Curci, M. Franzin, G. Decorti, G. Stocco, Inflammatory Bowel Disease and Risk of Colorectal Cancer: An Overview From Pathophysiology to Pharmacological Prevention, Front. Pharmacol. 12 (2021). https://doi.org/10.3389/fphar.2021.772101.

[26] J.-Y. Liu, X.-X. Hou, Z.-Y. Li, S.-H. Shan, M.-C. Chang, C.-P. Feng, Y. Wei, Isolation and structural characterization of a novel polysaccharide from Hericium erinaceus fruiting bodies and its arrest of cell cycle at S-phage in colon cancer cells, Int. J. Biol. Macromol. 157 (2020) 288–295. https://doi.org/10.1016/j.ijbiomac.2020.04.162.

[27] L. Ma, G.B. Xu, X. Tang, C. Zhang, W. Zhao, J. Wang, H. Chen, Anti-cancer potential of polysaccharide extracted from hawthorn (*Crataegus*.) on human colon cancer cell line HCT116 via cell cycle arrest and apoptosis, J. Funct. Foods 64 (2020) 103677. https://doi.org/10.1016/j.jff.2019.103677.

[28] G. Rona, B. Miwatani-Minter, Q. Zhang, H.V. Goldberg, M.A. Kerzhnerman, J.B. Howard, D. Simoneschi, E. Lane, J.W. Hobbs, E. Sassani, A.A. Wang, S. Keegan, D.J. Laverty, C.G. Piett, L.S. Pongor, M.L. Xu, J. Andrade, A. Thomas, P. Sicinski, M. Askenazi, B. Ueberheide, D. Fenyö, Z.D. Nagel, M. Pagano, CDK-independent role of D-type cyclins in regulating DNA mismatch repair, Mol. Cell 84 (2024) 1224-1242.e13. https://doi.org/10.1016/j.molcel.2024.02.010.

[29] S.F. Mansilla, M.B. De La Vega, N.L. Calzetta, S.O. Siri, V. Gottifredi, CDK-Independent and PCNA-Dependent Functions of p21 in DNA Replication, Genes 11 (2020) 593. https://doi.org/10.3390/genes11060593.

[30] Y. Pei, J. Yin, J. Liu, D. Liu, Q. Wu, X. Cai, M. Han, Y. Tian, L. Yang, S. Liu, The role of *NRF2* in human cancers: Pre-clinical insights paving the way for clinical trials, J. Pharm. Anal. (2025) 101358. https://doi.org/10.1016/j.jpha.2025.101358.

[31] J. Wang, B. Luo, X. Li, W. Lu, J. Yang, Y. Hu, P. Huang, S. Wen, Inhibition of cancer growth in vitro and in vivo by a novel ROS-modulating agent with ability to eliminate stem-like cancer cells, Cell Death Dis. 8 (2017) e2887–e2887. https://doi.org/10.1038/cddis.2017.272.

[32] S. Wei, Z. Yu, R. Shi, L. An, Q. Zhang, Q. Zhang, T. Zhang, J. Zhang, H. Wang, GPX4 suppresses ferroptosis to promote malignant progression of endometrial carcinoma via transcriptional activation by ELK1, BMC Cancer 22 (2022) 881. https://doi.org/10.1186/s12885-022-09986-3.

[33] M. Gao, Z. Qi, M. Deng, H. Huang, Z. Xu, G. Guo, J. Jing, X. Huang, M. Xu, J.A. Kloeber, S. Liu, J. Huang, Z. Lou, J. Han, The deubiquitinase USP7 regulates oxidative stress through stabilization of HO-1, Oncogene 41 (2022) 4018–4027. https://doi.org/10.1038/s41388-022-02403-w.

[34] N.A. Gandini, E.N. Alonso, M.E. Fermento, M. Mascaró, M.C. Abba, G.P. Coló, J. Arévalo, M.J. Ferronato, J.A. Guevara, M. Núñez, P. Pichel, A.C. Curino, M.M. Facchinetti, Heme Oxygenase-1 Has an Antitumor Role in Breast Cancer, Antioxid. Redox Signal. 30 (2019) 2030–2049. https://doi.org/10.1089/ars.2018.7554.

[35] R. Wei, Y. Zhao, J. Wang, X. Yang, S. Li, Y. Wang, X. Yang, J. Fei, X. Hao, Y. Zhao, L. Gui, X. Ding, Tagitinin C induces ferroptosis through PERK-Nrf2-HO-1 signaling pathway in colorectal cancer cells, Int. J. Biol. Sci. 17 (2021) 2703–2717. https://doi.org/10.7150/ijbs.59404.

[36] S. Jiang, H. Li, L. Zhang, W. Mu, Y. Zhang, T. Chen, J. Wu, H. Tang, S. Zheng, Y. Liu, Y. Wu, X. Luo, Y. Xie, J. Ren, Generic Diagramming Platform (GDP): a comprehensive database of high-quality biomedical graphics, Nucleic Acids Res. 53 (2025) D1670–D1676. https://doi.org/10.1093/nar/gkae973.

[37] C. Zhang, L. Li, J. Lin, J. Luo, L. Liu, X. Peng, Barley polysaccharides inhibit colorectal cancer by two relatively independent pathways, Int. J. Biol. Macromol. 277 (2024) 133820. https://doi.org/10.1016/j.ijbiomac.2024.133820.

[38] J. Luo, Q. Yang, W. Jiang, Y. Liu, Q. Hu, X. Peng, The interaction between *Angelica sinensis* polysaccharide ASP-2pb and specific gut bacteria alleviates rheumatoid arthritis in rats, Int. J. Biol. Macromol. 301 (2025) 140473. https://doi.org/10.1016/j.ijbiomac.2025.140473.

[39] C.C. Wong, J. Yu, Gut microbiota in colorectal cancer development and therapy, Nat. Rev. Clin. Oncol. 20 (2023) 429–452. https://doi.org/10.1038/s41571-023-00766-x.